Journal of Multidisciplinary Engineering Science Studies (JMESS)
ISSN: 2458-925X
Vol. 6 Issue 5, May - 2020

Comparison Of Signal Strength-Based And Distance-Based Cluster Head Selection For Cellular Network In The 2100 Mhz Frequency Band

Kufre M. Udofia
Department of Electrical/Electronic and Computer Engineering, University of Uyo, Nigeria

kmudofia@uniuyo.edu.ng

Abstract— In this paper, comparison of signal strength-based and distance-based cluster head selection for cellular network in the 2100 MHz frequency band is presented. The cluster head selection was done using Self-Organizing Map (SOM) clustering algorithm. The cluster head selection was first conducted with distance of the devices from the sink node (base station) as the key parameter and then, the cluster head selection is repeated with received signal strength as the key parameters. Specifically, a set of 100 devices located in a 1 km by 1 km area is considered in the study and the sink (base station is located at the centre of the area (where the centre coordinates are x= 0.5 km and y = 0.5 km). The range of values used for the selection of the cluster heads for distance d_k and received signal strength intensity (RSSI) are: $200\ \text{m} \leq d_k \leq 800\text{m}$ and $-80\ \text{dB} \leq RSSI_k \leq -66\ \text{dB}$ respectively. The results of the cluster head selection performed with the SOM algorithm based on distance show that only 16 cluster heads were selected from the 100 devices. The results of the cluster head selection performed with the SOM algorithm based on RSSI show that only 4 cluster heads were selected from the 100 devices. The results showed that the choice of parameters and the threshold values used for the parameter can significantly affect the outcome of the cluster head selection by SOM clustering algorithm.

Keywords— Clustering, Device-to-Device Communication, Self-Organizing Map (SOM), Cellular Network, Clustering Algorithm Signal Strength-Based Cluster Head Selection, Distance-Based Cluster Head Selection

1. Introduction

Today, different clustering algorithms are employed in the cluster head selection for the implementation of device-to-device (D2D) communication technologies [1-6]. This has become necessary, as researches have shown that D2D communication can be used to achieve energy efficiency in wireless communication networks [7-11].

Generally, the D2D technologies try to minimize the overall transmission energy demand in a network by allowing neighbouring nodes to relay their signals through a given node regarded as the cluster head [12-16]. The cluster heads are expected to have sufficient received signal strength and possible adequate hardware capacity. The focus on existing studies has been on the types of cluster heads and combinations of cluster head selection parameters. Most often, the cluster selection has been based on the location coordinates of the devices from the base station or the relative distance of the devices from the base station. The general assumption is that the RSSI is related to the relative distance (d) of the device to the base station. However, in reality the RSSI varies in different ways with distance depending on the path loss model and other loss parameter models that are used in the computation of the RSSI.

Researchers have shown that RSSI depends on a number of factors that include pathloss [17-27], obstruction [28,29], atmospheric conditions [30-37], terrain parameters, climatic parameters [38-42], among others. Accordingly, the use of distance instead of RSSI in the cluster head selection is re-evaluated in this paper. Specifically, the cluster head selection based on distance is compared with the cluster head selection based on RSSI. The key mathematical equations are given and SOM clustering algorithm is used in Matrix Laboratory (MATLAB) software for the cluster head selection.

2. Methodology

In this paper, the SOM cluster head selection for a set of devices in a cellular network coverage area is presented. The cluster head selection is first conducted with distance of the devices from the sink node (base station) as the key parameter and then, the cluster head selection is repeated with received signal strength as the key parameters. Specifically, a set of 100 devices located in a 1 km by 1 km area is considered in the study and the sink (base station is located at the centre of the area (where the centre coordinates are x= 0.5 km and y = 0.5 km).

$$d_k = \sqrt[2]{(x_k - x_0)^2 + (y_k - y_0)^2} \quad (1)$$

Where d_k is the distance of device k from the sink node; x_k , y_k are the coordinates of device k (node k) while x_0 , y_0 are the coordinates of sink node.

Again, for each device k, the RSSI with respect to free space path loss is given as [43-45];

$$RSSI_k = \text{EIRP}–PL_{FSPL\,(k)}(\text{dB}) = \text{EIRP}–32.44 - 20\log(\text{f}) - 20\log(d_k) \quad (2)$$

Where EIRP represented the effective isotropic radiated power expressed in dBW, and f = 2100 MHz.

3. Results and Discussion

The random function in MATLAB was used to generate the x_k , y_k are the coordinates of devices for k = 0,1,2,…, 100. Then, the d_k, $PL_{FSPL\,(k)}$ and $RSSI_k$ were computed in the MATLAB and the results are shown in Table 1. The plot of the x-coordinates and y-coordinates of the cellular devices around the sink (base station at the centre) is shown in Figure 1. In Figure 1, a region marked by $200\,m \leq d_k \leq 800m$ are selected for cluster heads. In essence, only

devices (node) that are in the given range of distance from the base station can be considered by the SOM algorithm in the selection of cluster heads. Nodes outside this range are not considered and hence they cannot be among the cluster heads. The pathloss obtained is for the devices are plotted and shown in Figure 2 while the RSSI are shown in Figure 3. The receiver sensitivity in the network is assumed to be -80 dB. As such, in Figure 3, the range of RSSI used for cluster head is $-70\ db \leq RSSI_k \leq -66\ dB$.

Table 1: The randomly generated x_k , y_k along with the d_k, $PL_{FSPL\,(k)}$ and $RSSI_k$ computed in MATLAB for the 100 devices

Device Number	x-coordinate (x_k) in m	y-coordinate (y_k) in m	Resultant Distance (d_k) in m	Pathloss ($PL_{FSPL\,(k)}$) in dB	Received Signal Strength Intensity ($RSSI_k$) in dBm
1	428.6	253.97	498.19	152.89	-99.392
2	605.17	985.7	1156.6	160.21	-106.71
3	440.87	766.1	883.89	157.87	-104.37
4	98.186	455.9	466.35	152.32	-98.819
5	398.05	567.21	692.94	155.76	-102.26
6	323.07	381.54	499.95	152.92	-99.423
7	807.65	271.17	851.96	157.55	-104.05
8	300.25	834.75	887.1	157.9	-104.4
9	681.75	647.09	939.95	158.41	-104.91
10	505.16	540.16	739.57	156.32	-102.82
11	22.625	3.7616	22.936	126.15	-72.655
12	986.61	227.9	1012.6	159.05	-105.55
13	772.92	337.92	843.56	157.47	-103.97
14	386.34	203.26	436.55	151.75	-98.245
15	855.42	432.2	958.4	158.58	-105.08
16	742.62	872.89	1146	160.13	-106.63
17	601.3	824.98	1020.9	159.12	-105.62
18	635.33	685.55	934.68	158.36	-104.86
19	222.62	914.81	941.5	158.42	-104.92
20	723.11	281.39	775.93	156.74	-103.24
21	212.28	150.93	260.47	147.26	-93.759
22	403.32	41.953	405.49	151.1	-97.604
23	339.26	112.07	357.29	150	-96.505
24	803.35	77.045	807.03	157.08	-103.58
25	183.31	501.18	533.65	153.49	-99.99
26	55.543	907.97	909.67	158.12	-104.62
27	807.96	746.41	1100	159.77	-106.27
28	849.14	131.55	859.27	157.63	-104.13
29	634.25	695.12	940.99	158.42	-104.92
30	991.72	756.25	1247.2	160.86	-107.36
31	925.16	984.83	1351.2	161.56	-108.06
32	911.9	837.46	1238.1	160.8	-107.3

33	102.08	974.93	980.26	158.77	-105.27
34	861.32	593.85	1046.2	159.34	-105.84
35	417.87	959.2	1046.3	159.34	-105.84
36	99.484	147.52	177.93	143.95	-90.449
37	953.15	259.68	987.89	158.84	-105.34
38	992.11	185.49	1009.3	159.02	-105.52
39	597.19	199.33	629.58	154.93	-101.43
40	791.9	103.83	798.68	156.99	-103.49
41	349.41	26.852	350.44	149.84	-96.337
42	243.83	105.38	265.63	147.43	-93.93
43	339.85	716.88	793.36	156.93	-103.43
44	745.29	732.7	1045.1	159.33	-105.83
45	546.62	608.22	817.75	157.2	-103.7
46	841.09	695.98	1091.7	159.71	-106.21
47	294.76	54.321	299.73	148.48	-94.979
48	897.43	356.86	965.78	158.64	-105.14
49	802.79	516.26	954.46	158.54	-105.04
50	207.35	332.83	392.13	150.81	-97.313
51	42.027	819.78	820.86	157.23	-103.73
52	107.61	502.1	513.51	153.16	-99.655
53	808.78	947.97	1246.1	160.86	-107.36
54	915.15	843.07	1244.3	160.84	-107.34
55	117.34	263.09	288.07	148.13	-94.634
56	669.39	123.04	680.6	155.6	-102.1
57	526.35	734.5	903.62	158.06	-104.56
58	123.73	211.3	244.86	146.72	-93.223
59	782.56	664.29	1026.5	159.17	-105.67
60	280.19	319.53	424.97	151.51	-98.012
61	47.453	690.19	691.82	155.74	-102.24
62	305.19	979.26	1025.7	159.16	-105.66
63	322.38	634.32	711.54	155.99	-102.49
64	479.87	698.31	847.3	157.51	-104.01
65	867.48	447.44	976.07	158.73	-105.23
66	514.37	460.95	690.69	155.73	-102.23
67	314.81	242.45	397.35	150.93	-97.428
68	728.57	684.47	999.65	158.94	-105.44
69	630.24	973.67	1159.8	160.23	-106.73
70	608.38	287.67	672.97	155.5	-102
71	997.72	277.89	1035.7	159.25	-105.75
72	16.69	520.86	521.13	153.28	-99.783
73	725.85	880.94	1141.4	160.09	-106.59

74	429.86	282.73	514.51	153.17	-99.672
75	871.22	751.34	1150.5	160.16	-106.66
76	967.89	524.7	1101	159.78	-106.28
77	414.98	414.72	586.69	154.31	-100.81
78	753.12	853.96	1138.6	160.07	-106.57
79	614.41	439.17	755.23	156.51	-103.01
80	945.27	766.3	1216.9	160.65	-107.15
81	962.66	10.988	962.72	158.61	-105.11
82	530.51	452.42	697.23	155.81	-102.31
83	602.56	765.81	974.45	158.72	-105.22
84	660.67	489.85	822.46	157.25	-103.75
85	6.0076	178.42	178.52	143.98	-90.478
86	99.436	399.95	412.12	151.24	-97.745
87	215.82	907.79	933.09	158.34	-104.84
88	83.398	492.03	499.05	152.91	-99.407
89	599.9	775.62	980.55	158.77	-105.27
90	849.08	622.22	1052.7	159.39	-105.89
91	478.53	286.95	557.98	153.88	-100.38
92	722.9	174.59	743.69	156.37	-102.87
93	320.85	659.25	733.18	156.25	-102.75
94	939.9	544.99	1086.5	159.66	-106.16
95	742.62	123.17	752.76	156.48	-102.98
96	11.525	848.1	848.18	157.51	-104.01
97	461.26	394.48	606.93	154.61	-101.11
98	826.55	15.87	826.7	157.29	-103.79
99	606.56	871.36	1061.7	159.46	-105.96
100	540.96	709.93	892.55	157.96	-104.46

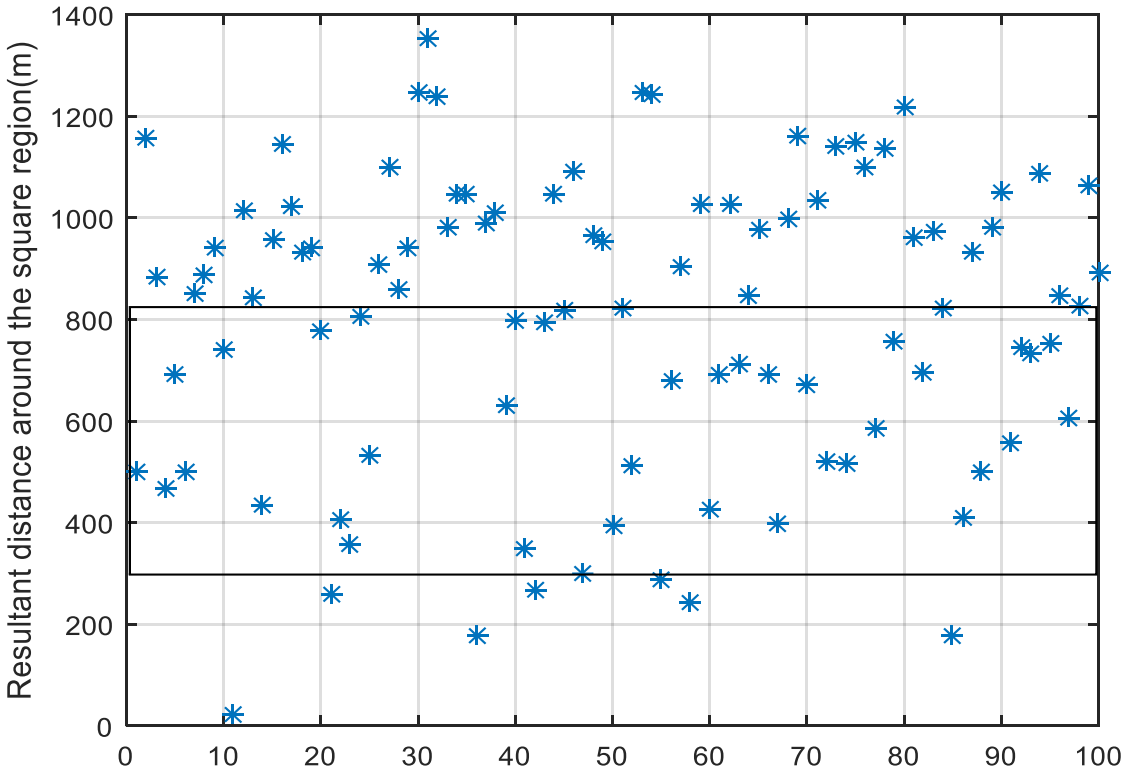

Figure 1: Plot showing the threshold for the devices considered as cluster head which are those occupying the distance between 200 m and 800 m from the sink node

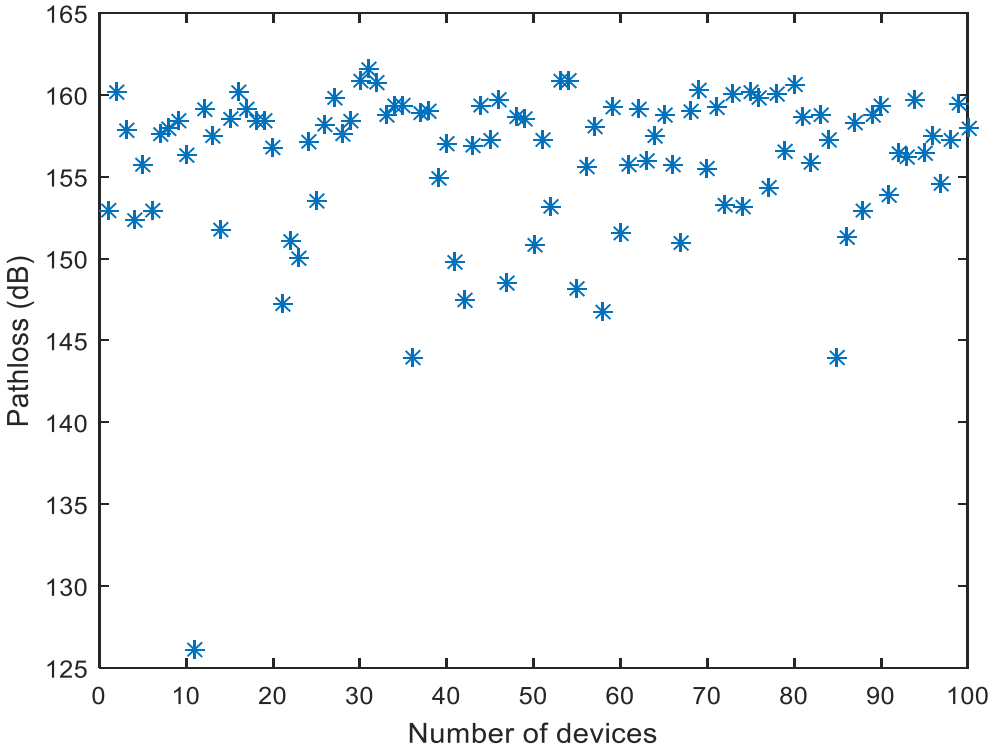

Figure 2: Plot showing pathloss of each of the devices.

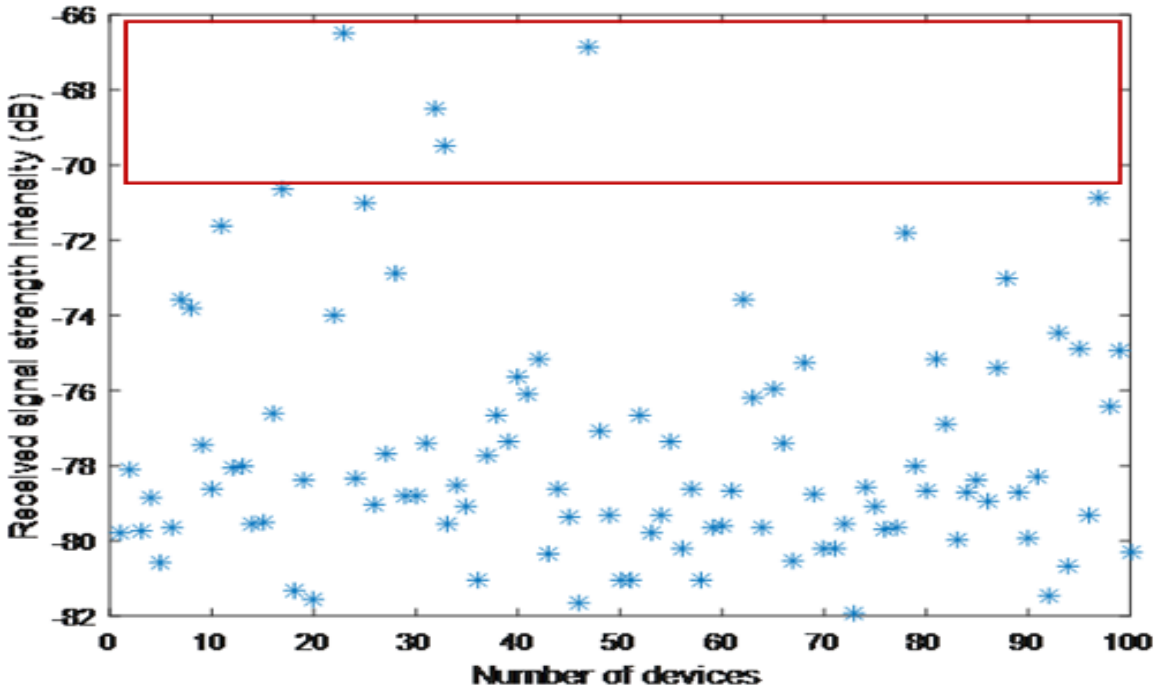

Figure 3: Plot showing the RSSI for each of the devices.

The outcome of the cluster head selection performed with the SOM algorithm based on distance, is shown in Figure 4 and Table 2 with the device number indicated on each of the cluster heads. The result of the clustering of the slave nodes to the 16 cluster heads with SOM algorithm is shown in Figure 5.

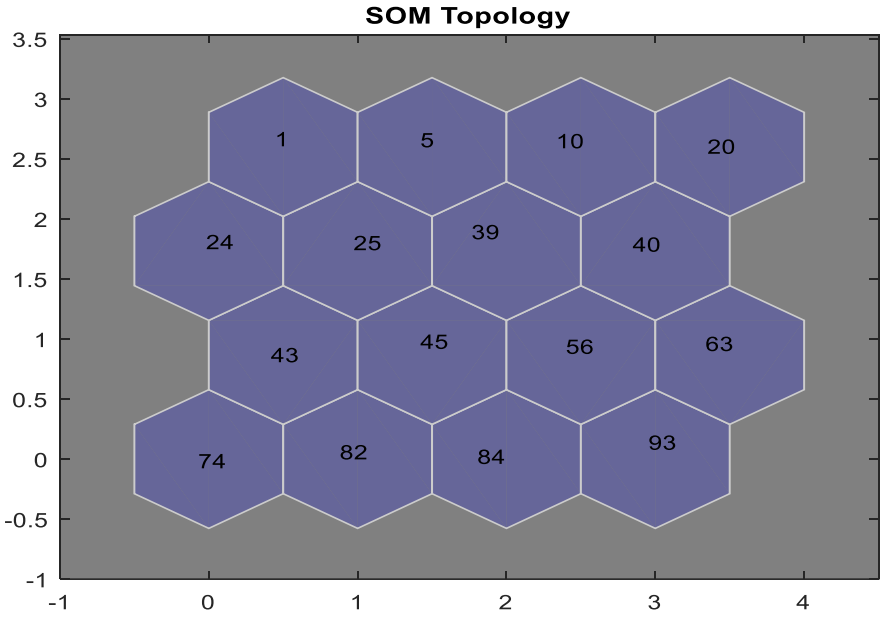

Figure 4: The outcome of the cluster head selection performed with the SOM algorithm based on distance showing that 16 cluster heads are selected.

Table 2: The outcome of the cluster head selection performed with the SOM algorithm based on distance showing that 16 cluster heads are selected

Device number	x-coordinates (m)	y-coordinates (m)	Resultant distance (m)	Pathloss (dB)	RSSI (dBm)
1	428.6	253.97	498.2	152.89	-99.392

5	398.05	567.21	692.94	155.76	-102.26
10	505.16	540.16	739.57	156.32	-102.82
20	222.62	914.81	941.51	158.42	-103.24
24	803.35	77.045	807.04	157.08	-103.58
25	183.31	501.18	533.65	153.49	-99.99
39	597.19	199.33	629.58	154.93	-101.43
40	791.9	103.83	798.68	156.99	-103.49
43	339.85	716.88	793.36	156.93	-103.43
45	546.62	608.22	817.76	157.2	-103.7
56	669.39	123.04	680.6	155.6	-102.1
63	322.38	634.32	711.54	155.99	-102.49
74	429.86	282.73	514.51	153.17	-99.672
82	530.51	439.17	697.23	155.81	-102.31
84	660.67	489.85	822.46	157.25	-103.75
93	320.85	659.25	733.18	156.25	-102.75

The clustering of the cluster heads to the cluster slaves performed by the clustering algorithm is shown in Figure 5.

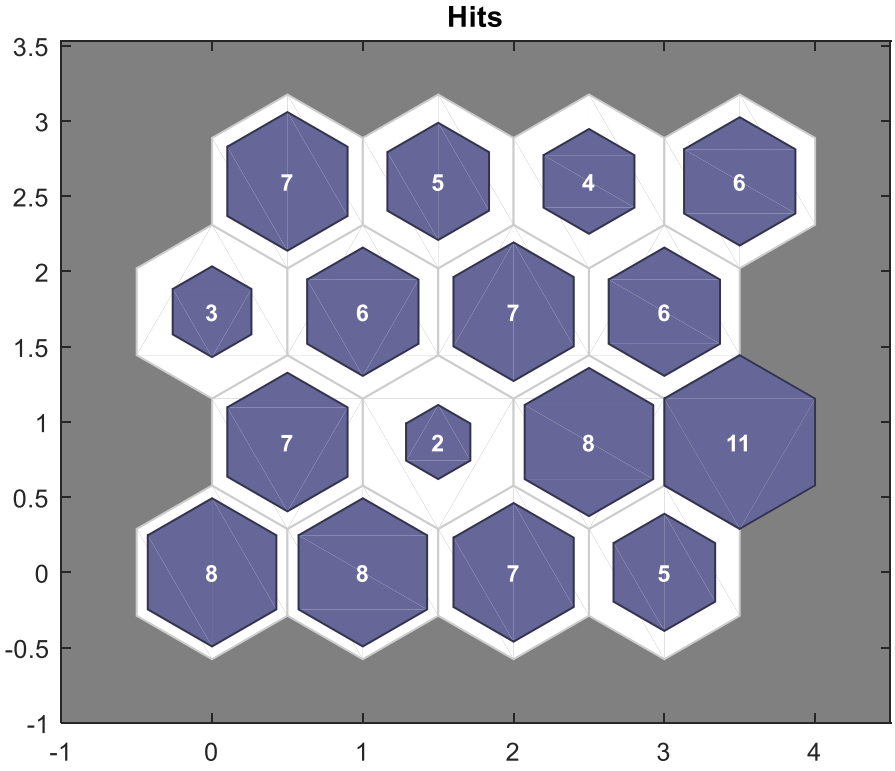

Figure 5: The result of the clustering of the slave nodes to the 16 cluster heads with SOM algorithm.

The outcome of the cluster head selection performed by the SOM algorithm based on RSSI, is shown in Figure 6 and Table 3 with the device number indicated on each of the cluster heads. The result of the clustering of the slave nodes to the 4 cluster heads with SOM algorithm is shown in Figure 7.

In all, with the RSSI, only 4 cluster heads were selected by the SOM algorithm, whereas sixteen 4 cluster heads were selected by the SOM algorithm when distance was used as the key selection parameter. The results showed that, the choice of parameters and the threshold used for the parameter can significantly affect the outcome of the cluster head selection by SOM clustering algorithm.

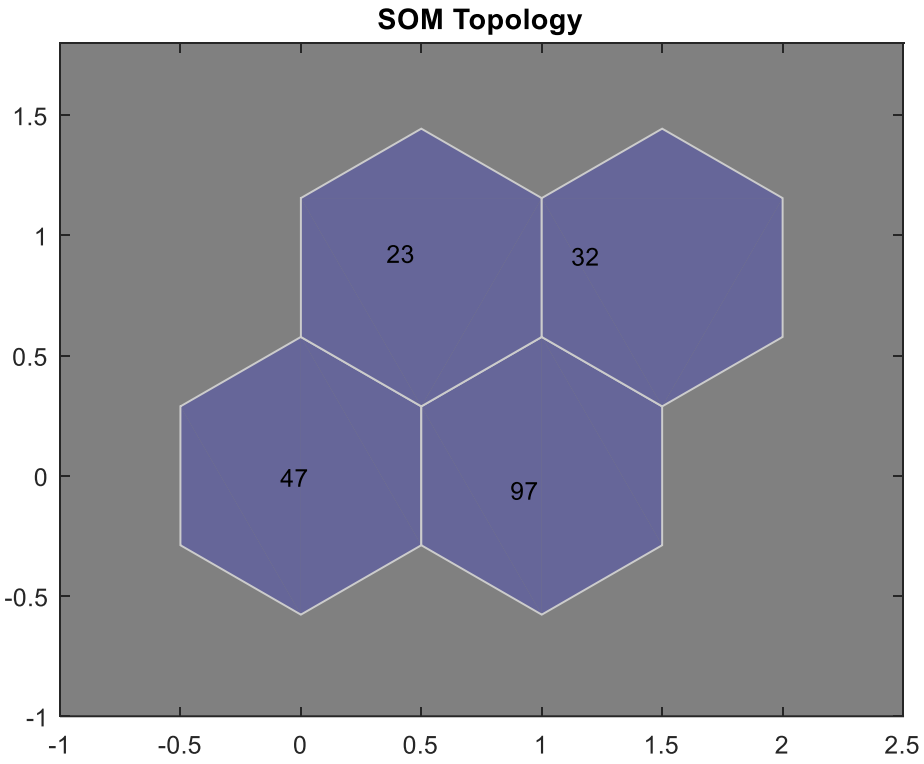

Figure 6: The outcome of the cluster head selection performed with the SOM algorithm based on RSSI showing that sixteen 4 cluster heads are selected.

Table 3: The outcome of the cluster head selection performed with the SOM algorithm based on RSSI showing that 4 cluster heads are selected.

Device number	x-coordinates (m)	y-coordinates (m)	Resultant distance (m)	Pathloss (dB)	RSSI (dBm)
23	87.5003	99.0953	132.1975	141.3689	-66.4666
32	21.6498	178.9825	180.2871	144.0637	-68.5051
47	29.9920	137.5466	140.7785	141.9151	-66.8798
97	217.7321	138.6017	258.1040	147.1803	-70.8625

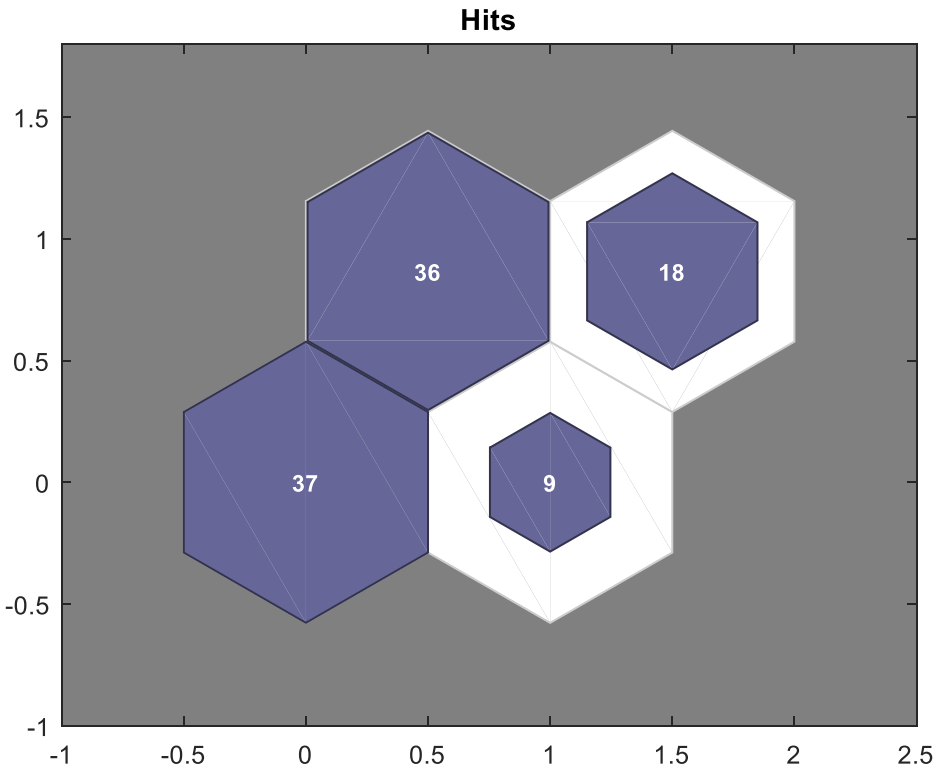

Figure 7: The result of the clustering of the slave nodes to the 4 cluster heads with SOM algorithm based on RSSI.

In all, with the RSSI, only 4 cluster heads were selected by the SOM algorithm, whereas 16 cluster heads were selected by the SOM algorithm when distance was used as the key selection parameter. The results showed that, the choice of parameters and the threshold used for the parameter can significantly affect the outcome of the cluster head selection by SOM clustering algorithm.

4. Conclusion

The effect of cluster head selection parameter on the Self-organizing map clustering algorithm employed in device-to-device communication in cellular network is presented. First, the SOM algorithm was employed to select cluster heads based on the distance of the device from the base station. Next, the cluster head selection was conducted using RSSI as the key parameter. The results showed that the number of cluster heads selected with the RSSI is lower than that selected with the distance as the key parameter. It was concluded that the selection parameter and especially the threshold values used for each of the selection parameters do affect the SOM algorithm outcome in a significant way.

References

1. Sharafeddine, Sanaa, and Omar Farhat. "A proactive scalable approach for reliable cluster formation in wireless networks with D2D offloading." *Ad Hoc Networks* 77 (2018): 42-53.
2. Paramonov, Alexander, et al. "Clustering optimization for out-of-band D2D communications." *Wireless Communications and Mobile Computing* 2017 (2017).
3. Li, Yuhong, et al. "A cluster-based routing method for D2D communication oriented to vehicular networks." *2017 IEEE International Conference on Systems, Man, and Cybernetics (SMC)*. IEEE, 2017.
4. Zhao, Yifeng, et al. "Distributed dynamic cluster-head selection and clustering for massive IoT access in 5G networks." *Applied Sciences* 9.1 (2019): 132.
5. Doumiati, Salam, Hassan Artail, and Karim Kabalan. "A framework for clustering LTE devices for implementing group D2D communication and multicast capability." *2017 8th International Conference on Information and Communication Systems (ICICS)*. IEEE, 2017.
6. Fodor, Gabor, et al. "Device-to-device communications for national security and public safety." *IEEE Access* 2 (2014): 1510-1520.
7. Shang, Bodong, et al. "Energy-efficient device-to-device communication in cellular networks." *2016 IEEE 83rd Vehicular Technology Conference (VTC Spring)*. IEEE, 2016.
8. Zabetian, Negar, Abbas Mohammadi, and Meysam Masoudi. "Energy-efficient power allocation for device-to-device communications underlaid cellular networks using stochastic geometry." *Transactions on Emerging*

Telecommunications Technologies 30.12 (2019): e3768.

9. Park, Hyebin, and Yujin Lim. "Reinforcement Learning for Energy Optimization with 5G Communications in Vehicular Social Networks." *Sensors* 20.8 (2020): 2361.
10. Della Penda, Demia. *Device-to-Device Communication in Future Cellular Networks: Resource allocation and mode selection*. Diss. Kungliga Tekniska högskolan, 2018.
11. Ali, Kamran, et al. "Disaster management using D2D communication with power transfer and clustering techniques." *IEEE Access* 6 (2018): 14643-14654.
12. Yaacoub, Elias, et al. "On the impact of D2D traffic offloading on energy efficiency in green LTE-A HetNets." *Wireless Communications and Mobile Computing* 15.6 (2015): 1089-1105.
13. Amodu, Oluwatosin Ahmed, et al. "Relay-assisted D2D underlay cellular network analysis using stochastic geometry: Overview and future directions." *IEEE Access* 7 (2019): 115023-115051.
14. Kar, Udit Narayana, and Debarshi Kumar Sanyal. "An overview of device-to-device communication in cellular networks." *ICT express* 4.4 (2018): 203-208.
15. Zhou, Kai, Jinsong Gui, and Naixue Xiong. "Improving cellular downlink throughput by multi-hop relay-assisted outband D2D communications." *EURASIP Journal on Wireless Communications and Networking* 2017.1 (2017): 1-23.
16. Sun, Weifeng, et al. "A survey of using swarm intelligence algorithms in IoT." *Sensors* 20.5 (2020): 1420.
17. Aloziem, Njoku Chukwudi, Ozuomba Simeon, and Afolayan J. Jimoh. "Tuning and Cross Validation of Blomquist-Ladell Model for Pathloss Prediction in the GSM 900 Mhz Frequency Band." *International Journal of Theoretical and Applied Mathematics* 3.2 (2017): 94.
18. Pu, Chuan Chin, Pei Cheng Ooi, and Wan-Young Chung. "Accuracy and stability analysis of path loss exponent measurement for localization in wireless sensor network." *International Journal of Digital Content Technology and its Applications* 7.7 (2013): 1148-1156.
19. Liechty, Lorne Christopher. *Path loss measurements and model analysis of a 2.4 GHz wireless network in an outdoor environment*. Diss. Georgia Institute of Technology, 2007.
20. Obot, A., O. Simeon, and J. Afolayan. "Comparative analysis of path loss prediction models for urban macrocellular environments." *Nigerian journal of technology* 30.3 (2011): 50-59.
21. Goshwe, N. Y., J. Orinya, and G. A. Igwue. "Prediction of Path loss Estimate for a Frequency Modulation (FM) Station Using Basic Transmission Loss Model." *Global Journal of Engineering Research* 12 (2013): 69-75.
22. Han, Seon Yeong, Nael B. Abu-Ghazaleh, and Dongman Lee. "Efficient and consistent path loss model for mobile network simulation." *IEEE/ACM Transactions on Networking* 24.3 (2015): 1774-1786.
23. Ozuomba, Simeon., Enyenihi, Johnson., & Rosemary, N. Chinyere. (2018). Characterisation of Propagation Loss for a 3G Cellular Network in a Crowded Market Area Using CCIR Model. *Review of Computer Engineering Research*, *5*(2), 49-56.
24. Seidel, Scott Y., and Theodore S. Rappaport. "914 MHz path loss prediction models for indoor wireless communications in multifloored buildings." *IEEE transactions on Antennas and Propagation* 40.2 (1992): 207-217.
25. Yamamoto, Brennan, et al. "Received signal strength indication (RSSI) of 2.4 GHz and 5 GHz wireless local area network systems projected over land and sea for near-shore maritime robot operations." *Journal of Marine Science and Engineering* 7.9 (2019): 290.
26. Akaninyene B. Obot , Ozuomba Simeon and Kingsley M. Udofia (2011); *"Determination Of Mobile Radio Link Parameters Using The Path Loss Models"* NSE Technical Transactions , A Technical Journal of The Nigerian Society Of Engineers, 46.2 (2011): 56-66.
27. Nadir, Zia, and M. Suwailam. "Pathloss Analysis at 900 MHz for Outdoor Environment." *Proceedings of the 2014 International Conference on Communications, Signal Processing and Computers,(EUROPMENT 2014)*. 2014.
28. Samuel, Wali, Fidelis Osanebi Chucks Nwaduwa, and Trust Christopher Oguichen. "Algorithm for Computing N Knife Edge Diffraction Loss Using Epstein-Peterson Method." *American Journal of Software Engineering and Applications* 6.2 (2017): 40-43.
29. Ozuomba, Simeon, Constant Kalu, and Henry Johnson Enyenihi. "Comparative Analysis of the Circle Fitting Empirical Method and the International Telecommunication Union Parabola Fitting Method for Determination of the Radius of Curvature for Rounded Edge Diffraction Obstruction." *Communications* 7: 16-21.
30. Mason, Samuel P. *Atmospheric effects on radio frequency (RF) wave propagation in a humid,*

near-surface environment. Naval Postgraduate School Monterey Ca, 2010.

31. Ozuomba, Simeon, Constance Kalu, and Akaninyene B. Obot. "Comparative Analysis of the ITU Multipath Fade Depth Models for Microwave Link Design in the C, Ku, and Ka-Bands." *Mathematical and Software Engineering* 2.1 (2016): 1-8.
32. Kaseta, S., V. Grimaila, and D. Rukavicius. "Experimental research of signal fading in fixed wireless links." *Elektronika ir Elektrotechnika* 20.4 (2014): 72-75.
33. Johnson, Enyenihi Henry, Simeon Ozuomba, and Kalu Constance. "Development of Model for Estimation of Radio Refractivity from Meteorological Parameters." (2019).
34. Eli-Chukwu, Ngozi Clara, and G. N. Onoh. "Experimental Study on the Impact of Weather Conditions on Wide Code Division Multiple Access Signals in Nigeria." *Eng. Technol. Appl. Sci. Res* 9.2 (2019): 3998-4001.
35. Luomala, Jari, and Ismo Hakala. "Effects of temperature and humidity on radio signal strength in outdoor wireless sensor networks." *2015 Federated Conference on Computer Science and Information Systems (FedCSIS)*. IEEE, 2015.
36. Onafuye, Olasunkanmi O., et al. "Adaptive Neuro-Fuzzy Inference System (Anfis) Model for Prediction of Vertical Profile of Radioclimatic Parameters." *European Journal of Engineering and Technology Vol* 6.5 (2018).
37. Dohnálek, Pavel, et al. "A signal strength fluctuation prediction model based on the random forest algorithm." *Elektronika ir Elektrotechnika* 20.5 (2014): 123-126.
38. Eunice, Akinloye Bolanle, Simeon Ozuomba, and Isaac A. Ezenugu. "Evaluation of the Distribution of Terrain Roughness Index for Terrestrial Line of Site Microwave Links in Uyo Metropolis." *Mathematical and Software Engineering* 2.1 (2016): 9-18.
39. Sarwar, Muhammad. "Effects of terrain features on wave propagation: high-frequency techniques." (2009).
40. Yamamoto, Brennan, et al. "Received signal strength indication (RSSI) of 2.4 GHz and 5 GHz wireless local area network systems projected over land and sea for near-shore maritime robot operations." *Journal of Marine Science and Engineering* 7.9 (2019): 290.
41. Ozuomba, Simeon, Henry Johnson Enyenihi, and Constance Kalu. "Program to Determine the Terrain Roughness Index using Path Profile Data Sampled at Different Moving Window Sizes." *International Journal of Computer Applications* 975: 8887.
42. Rao, T. Rama, et al. "Near Ground/Floor RF Path Gain Measurements in Indoor Corridors at 2400 MHz for Wireless Sensor Communications." *Procedia Engineering* 30 (2012): 836-843.
43. Emenyi, Mfon, Kufre Udofia, and Obinwa Christian Amaefule. "Computation of optimal path Length for terrestrial line of sight microwave link using Newton–Raphson algorithm." *Software Engineering* 5.3 (2017): 44.
44. Kalu, Constance. "Development and Performance Analysis of Bisection Method-Based Optimal Path Length Algorithm for Terrestrial Microwave Link." *Review of Computer Engineering Research* 6.1 (2019): 1-11.
45. Johnson, Enyenihi Henry, Simeon Ozuomba, and Ifiok Okon Asuquo. "Determination of Wireless Communication Links Optimal Transmission Range Using Improved Bisection Algorithm." (2019).